

L - 343

NATIONAL ADVISORY COMMITTEE FOR AERONAUTICS

WARTIME REPORT

ORIGINALLY ISSUED
September 1942 as
Advance [REDACTED] Report

THE EFFECT OF COWLING SHAPE ON THE STABILITY

CHARACTERISTICS OF AN AIRPLANE

By C. J. Donlan and W. Letko

Langley Memorial Aeronautical Laboratory
Langley Field, Va.



WASHINGTON

NACA WARTIME **REPORTS** are reprints of papers originally issued to provide rapid distribution of advance research results to an authorized group requiring them for the war effort. They were previously held under a security status but are now unclassified. Some of these reports were not technically edited. All have been reproduced without change in order to expedite general distribution.

NATIONAL ADVISORY COMMITTEE FOR AERONAUTICS

ADVANCE [REDACTED] REPORT

THE EFFECT OF COWLING SHAPE ON THE STABILITY
CHARACTERISTICS OF AN AIRPLANE

By C. J. Donlan and W. Letko

SUMMARY

Three widely different nose shapes were tested on a fuselage alone and on a complete model in the UACA stability tunnel to investigate the effect of cowl shape on stability characteristics. The results are presented in the form of charts which show the variation in the aerodynamic characteristics with the three nose shapes for the propeller-removed condition over a wide range of angles of attack and yaw.

The results of the investigation indicated that large changes in the cowl shape produced relatively small changes in the aerodynamic characteristics. The effects may be appreciable, however, in the case of an airplane that has marginal stability.

INTRODUCTION

The trend in contemporary airplane design toward higher wing loadings, smaller wing areas with respect to fuselage areas, and larger moments of inertia makes the attainment of satisfactory stability characteristics increasingly difficult (reference 1). Small changes in the stability parameters, therefore, may produce significant changes in the stability characteristics of the airplane. One common change made on existing airplanes is a modification of the engine cowl. Recent flight investigations have suggested that changes in the type or the shape of engine cowl may alter the flying qualities of an airplane, but little direct information is available concerning these effects. Pressure-distribution measurements over cowlings of various shapes are given in references 2, 3, and 4. Reference 2 contains data on cowlings over a considerable range of angles of attack but does not show

the effect of the cowling on the fuselage pressure distribution. References 3 and 4 contain extensive pressure-distribution measurements at low angles of attack on a number of cowlings-fuselage arrangements over a wide range of Mach numbers. Reference 5 shows the effect of a radial, engine and cowlings on the unstable moment of a streamline body but does not show the effect on the weathercock stability of the complete airplane. The present investigation was made to provide direct information concerning the effect of cowlings shape on the longitudinal- and lateral-stability characteristics of the entire airplane.

Two cowlings representing extremes in contemporary design practice were tested. In addition, a streamline nose section was tested to provide a basis for comparison. Arrangements were made also for varying the volume of air flowing through the cowlings. The propellers were not represented. Tests were made of a fuselage alone and of a complete model consisting of a fuselage, a wing, and horizontal and vertical tail surfaces.

The paper presents the aerodynamic characteristics in pitch and in yaw of the different combinations tested. The data must be used in a strictly comparative manner, inasmuch as no corrections for wind-tunnel wall effects or support-strut interference have been applied.

APPARATUS AND MODELS

The tests were made in the closed-throat NACA stability tunnel. This tunnel is of recent construction. At the outset of this investigation, the characteristics of neither the tunnel nor the balances had been explored very thoroughly; consequently, no attempt has been made to apply any corrections to the data obtained. In view of the comparative nature of the present investigation, however, this procedure should not qualify any of the conclusions reached.

The tunnel is equipped with a six-component balance especially designed to measure the forces and moments with respect to a system of axes commonly used in stability work. This system of axes is shown in figure 1. The orientation of the drag vector should be noted particularly.

The model used in this investigation is representa-

tive of a conventional single-engine military pursuit airplane equipped with a radial engine. A three-view drawing of the 0.1-scale airplane model showing the relative size and location of the streamline nose and the two cowlings is given in figure 2. Although no propeller was used, all nose sections were constructed in such a way that; the plane of the propeller was at a fixed distance from the center of gravity.

The model was constructed of laminated mahogany. All exposed surfaces were sprayed with lacquer and a smooth finish was obtained. Both cowlings were modeled after the cowlings used in the investigation reported in reference 6. Details of the test arrangement for the NACA open-nose and high-speed cowlings are given in figures 3 and 4, respectively.

In the NACA high-speed cowling, the cooling air enters at the nose of the forward element of the cowling. This element acts as a spinner and normally rotates with the propeller, the rotating element is fitted internally with cuffs that serve as fairings for the propeller-blade shanks. In the present investigation, no propeller was used and the rotating element was held rigid. The cowling exit arrangement was unconventional in that the cooling air was exhausted through two ducts, one on each side of the fuselage, instead of through the conventional annular exit at the cowling skirt.

The resistance offered by the engine to the air flowing through the cowlings was simulated by perforated plates, the conductances of which could be varied. For both cowlings, the condition of maximum conductance approximated the full-scale conductance of a typical single-row radial-engine installation without cowling flaps.

Typical test set-ups are shown in figure 5.

TESTS

The streamline nose and the two cowlings were each tested on the fuselage alone and on the complete model. Each combination was tested throughout the range of angle of attack from -5° to 18° at angles of yaw of -5° , 0° , and 5° . Tests were made also in which the angle of yaw was varied from 10° to -40° with the angle of attack fixed at 0° and 10° .

Most of the tests with the two cowlings were run in the condition representing maximum conductance. Some tests with the NACA open-nose cowling were, however, run with zero conductance; that is, the flow through the cowling was completely stopped.

The tests were made at a dynamic pressure of 65 pounds per square foot, which corresponds to a speed of about 160 miles per hour under standard conditions. The test Reynolds number based on the wing *chord* was about 888,000. Repeat tests were made at dynamic pressures of 100 and 125 pounds per square foot (corresponding to test Reynolds numbers of 1,190,000 and 1,338,000, respectively) but little scale effect was observed in this range.

PRESENTATION OF RESULTS

All data are reduced to nondimensional coefficients and are uncorrected for initial asymmetry in the model or air stream, for support-strut interference, and for wind-tunnel wall interference. All coefficients are referred to the system of axes shown in figure 1. The coefficients for the fuselage are based on the wing dimensions. The symbols and coefficients used in this report are defined as follows:

C_D	drag coefficient (D/qS)
C_L	lift coefficient (lift/qS)
C_Y	lateral-force coefficient (Y/qS)
C_m	pitching-moment coefficient (M/qSc)
C_l	rolling-moment coefficient (L/qSb)
C_n	yawing-moment coefficient (N/qSb)
D	drag (See fig. 1)
Y	lateral force
M	pitching moment
L	rolling moment

N	yawing moment
q	dynamic pressure ($\frac{1}{2}\rho V^2$)
V	tunnel air velocity
S	wing area
c	wing chord
K	conductance of cowling
α	angle of attack (thrust line)
ψ	angle of yaw
$C_{Y\psi}$	$\frac{\partial C_Y}{\partial \psi}$
$C_{l\psi}$	$\frac{\partial C_l}{\partial \psi}$
$C_{n\psi}$	$\frac{\partial C_n}{\partial \psi}$

The variation of the measured lift, drag, and pitching-moment coefficients with angle of attack for the different combinations tested is given in figures 6 to 8. The effect of yaw on these coefficients is illustrated in figure 9. Typical variations of the lateral-force coefficient, the rolling-moment coefficient, and the yawing-moment coefficient with angle of yaw are presented in figures 10 to 12.

The variation of the stability parameters C_Y , $C_{l\psi}$, and $C_{n\psi}$ with angle of attack is given in figures 13 and 14.

1.4. The parameters $C_{Y\psi}$, $C_{l\psi}$, and $C_{n\psi}$ represent the slope, at zero yaw, of the curves of the coefficients against angle of yaw. In figures 13 and 14 the tailed points are the measured slopes. The plain points were evaluated from the data taken at angles of yaw of $\pm 5^\circ$ by assuming a linear variation of the coefficients in this range. This method of computing the parameters yields results within the practical limits of accuracy for angles

of attack below the stall. For angles of attack above the stall, the parameters evaluated by this method have less significance.

DISCUSSION

A change in the type or the shape of the cowling on an airplane could affect the stability and control characteristics by virtue of the following effects:

1. A change in the force and moment contribution of the fuselage resulting from a redistribution of area and the altered basic pressure distribution over the fuselage. This pressure distribution is affected also by the conductance of the cowling - at least, over the portion of the fuselage occupied by the cowling. (See reference 4.)

2. Interference effects on the wing and the tail surfaces resulting from the altered flow pattern around the fuselage. These effects may also vary with the conductance of the cowling.

The extent of the effects attributable to changes in the basic pressure distribution can be determined from the results for the fuselage alone. A comparison of the results for the fuselage alone and the results for the complete model should reveal some of the effects attributable to interference. It is appreciated that the comparisons should be made on a relative basis; that is, a given change of moment coefficient is of greater importance in yaw than in pitch because the total moment coefficient is usually less.

Fuselage alone.- The data in figure 6 indicated that the different shapes tested had little effect on the characteristics of the fuselage in pitch. The parameter most affected was the drag coefficient. At high angles of attack the more blunt NACA open-nose cowling had the highest drag, caused possibly by an earlier breakdown of the flow over the cowling. A similar increase in drag is noticeable at an angle of yaw of 17° . (See fig. 9.)

The effect of the different noses on the lateral-stability characteristics should be noted (fig. 13). The fuselage with the NACA high-speed cowling gives values of $C_{Y\psi}$ about 0.0005 lower and values of $C_{n\psi}$ as much as

0.0003 more positive, that is, more unstable, than the corresponding parameters for the fuselage with the NACA open-nose cowling. It will be observed also that at large angles of yaw the fuselage with the NACA high-speed cowling developed considerably smaller lateral forces than the fuselage with the BACA open-nose cowling. These results are in agreement with the trends indicated in reference 5. In figure 10 the scatter of the rolling-moment coefficients is so great that no attempt was made to fair a curve through the points,

Complete model.— Apart from slight irregularities in the lift curve at an angle of attack of about 10° , the type of cowling affixed to the fuselage did not appreciably affect the characteristics in pitch of the complete model (figs. 7(a) and 7(b)). The effect of conductance should be noted (figs. 8(a) and 8(b)). With zero conductance, a breakdown of the flow probably occurs at a lower angle of attack. This condition is associated possibly with the development of critical peak pressures on the cowling at lower angles of attack as the conductance of the cowling is decreased. (See reference 4.)

The effect of the three nose shapes on the lateral-stability characteristics of the complete model (fig. 14) is similar to the effects observed on the fuselage alone. The values fluctuate somewhat with angle of attack but it is seen that, in the normal range of angle of attack, the value of $C_{Y\psi}$ for the NACA high-speed cowling is always less than the corresponding value for the NACA open-nose cowling and that $C_{n\psi}$ is always more positive, that is, more unstable, than the corresponding value of $C_{n\psi}$ for the NACA open-nose cowling. The actual increments in these parameters were of the same order of magnitude as those observed for the fuselage alone; that is, $\Delta C_{Y\psi} = -0.0005$ and $\Delta C_{n\psi} = 0.0003$. Check tests made of the fuselage in combination with the horizontal and vertical tail surfaces have verified these observations. The absolute differences, however, are small and, if plotted to the scale of figure 11, may be overlooked. In figure 14, fluctuations in the parameter C_l around 11° or 12° indicate that both wings do not stall simultaneously. The effect of conductance was not investigated very extensively but, at low angles of attack, it appeared to be small.

At large angles of yaw the results for the NACA open-nose cowling show larger lateral-force coefficients and larger yawing moments (fig 11). The favorable effect of the flow through the cowling on the rolling characteristics at angles of yaw beyond 15° is interesting.

The effect of the cowlings cannot be rigorously separated into changes resulting from the altered basic pressure distribution over the fuselage and changes resulting from interference effects on the flow over the wing and tail surfaces without complete data on all combinations of the wing, tail surfaces, and fuselage. It would appear from a comparison of the results for the fuselage alone and for the complete model, however, that a large percentage of the changes in the stability parameters were primarily attributable to the altered basic pressure distribution over the fuselage.

CONCLUSIONS

The results of this investigation admit the following conclusions concerning the effect of cowling shape on the stability characteristics of an airplane:

1,. Ordinary changes in the type or the shape of a cowling affixed to an airplane are apt to produce appreciable changes in the lateral-stability characteristics of the airplane only if the initial stability is marginal. In the present investigation a radical change in the shape of the cowling resulted in only a small reduction in weathercock stability.

2, Below the critical speed of the cowling, practical variations of engine conductance will have minor effects on the stability characteristics of the airplane, except possibly in the neighborhood of the stall.

Langley Memorial Aeronautical Laboratory,
National Advisory Committee for Aeronautics,
Langley Field, Va.

REFERENCES

1. Bamber, Millard J.: Effect of Some Present-Day Airplane Design Trends on Requirements for Lateral Stability. NACA TN No. 814, 1941.
2. Higginbotham, R. R.: Air Forces on Radial Air-Cooled Engine Cowling (as Determined from Pressure Distribution Tests) SAE Jour., vol. 47, no. 3, Sept. 1940, pp. 370-396.
3. Robinson, Russell G., and Becker, John V.: High-Speed Tests of Conventional Radial-Engine Cowlings. NACA Rep. No. 745, 1942.
4. Becker, John V.: Wind-Tunnel Tests of Air Inlet and Outlet Openings on a Streamline Body. NACA A.C.R., Nov. 1940.
5. Jacobs, Eastman N., and Ward, Kenneth E.: Interference of Wing and Fuselage from Tests of 209 Combinations in the N.A.C.A. Variable-Density Tunnel. NACA Rep. No. 540, 1935.
6. McHugh, James G.: Progress Report on Cowlings for Air-Cooled Engines Investigated in the NACA 19-Foot Pressure Wind Tunnel. NACA A.R.R., July 1941.

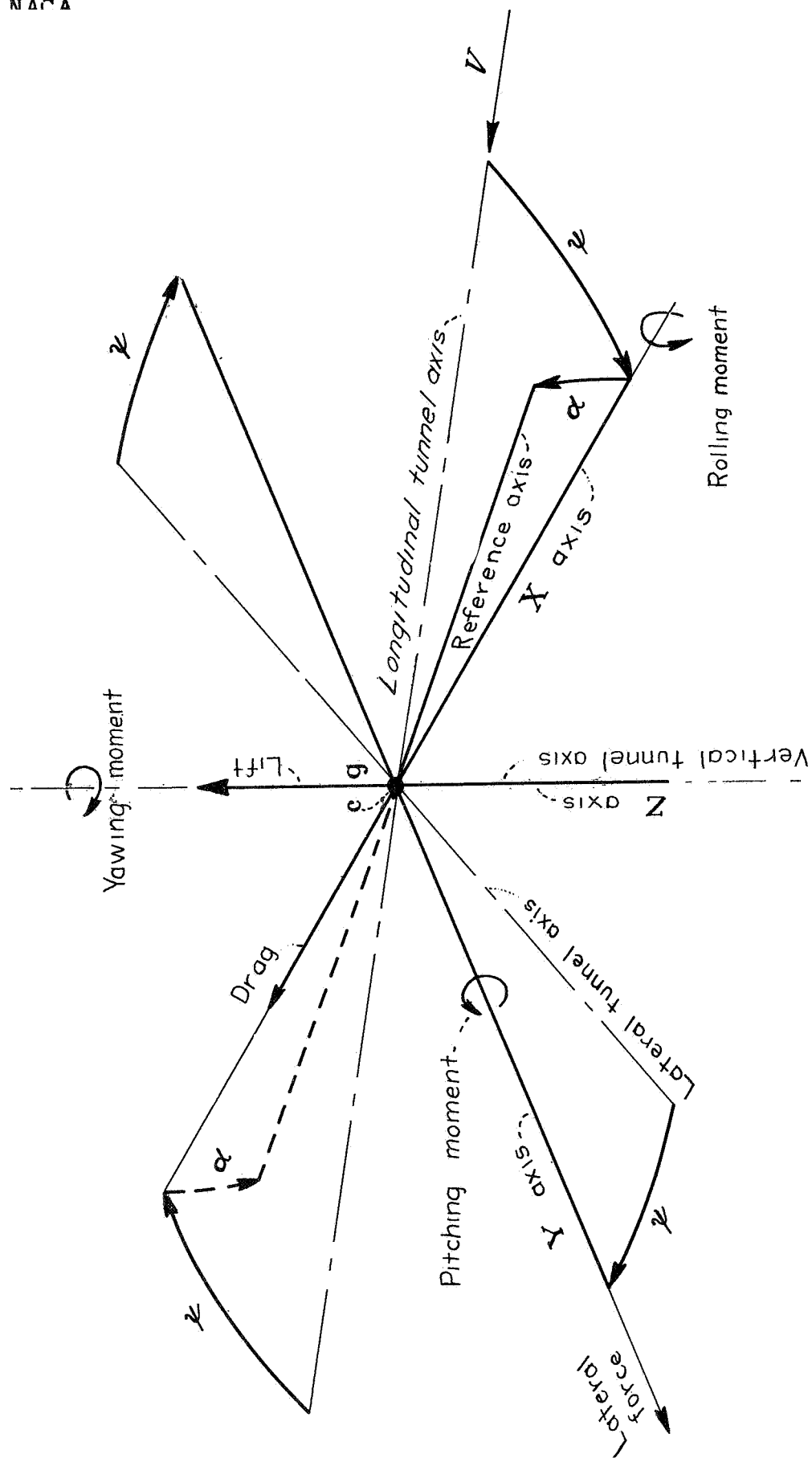


Figure 1.- System of axes used for force and moment measurements in the stability tunnel.

NACA

Wing area 361 sq in.
C.g. location 0.23 mean chord
Vertical tail area 38.16 sq in.
Horizontal tail area 79.20 sq in.

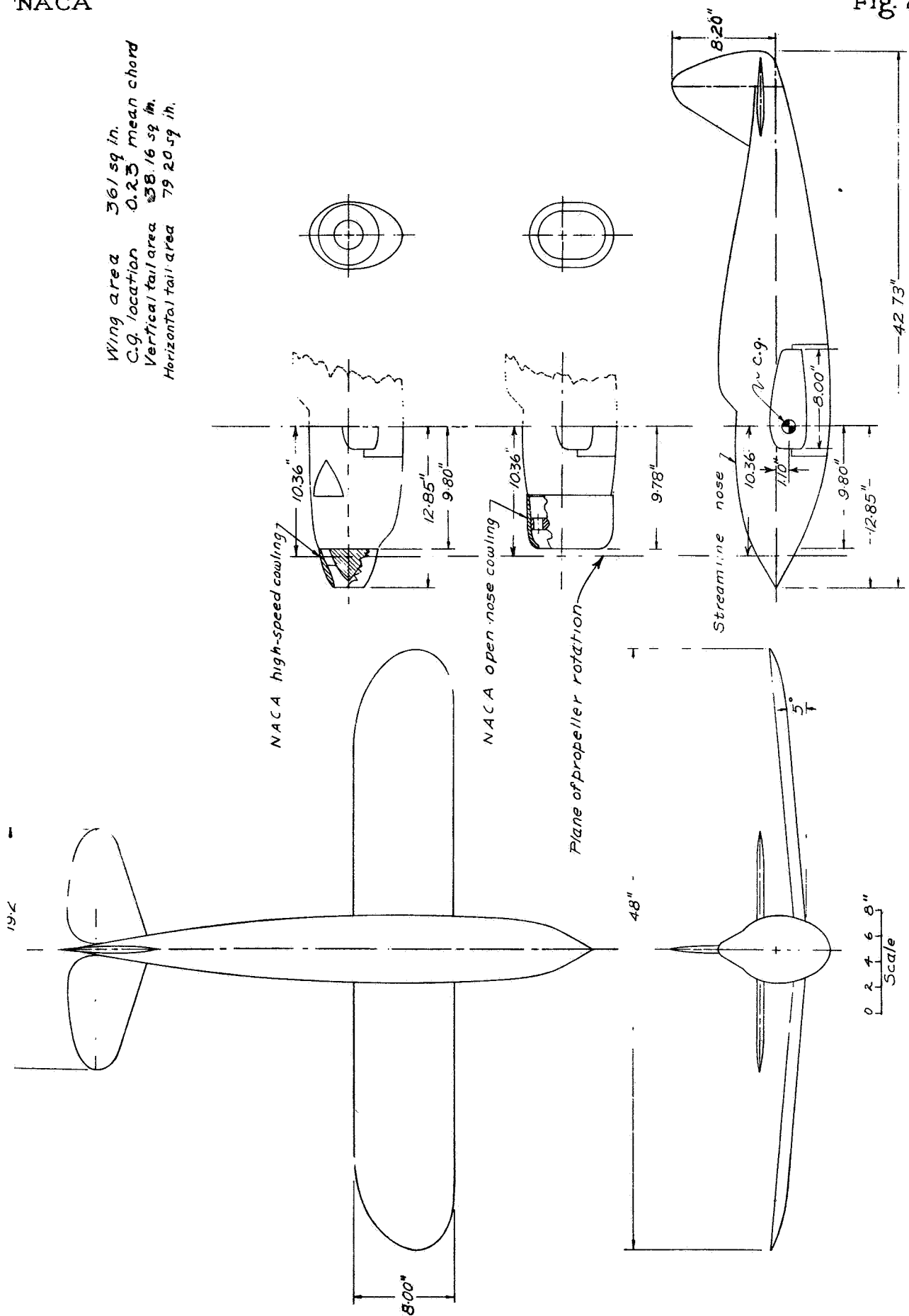


Fig. 2

Figure 2 - Three-view drawing of the 0.1-scale pursuit airplane model with three nose sections

NACA

Figs 3,4

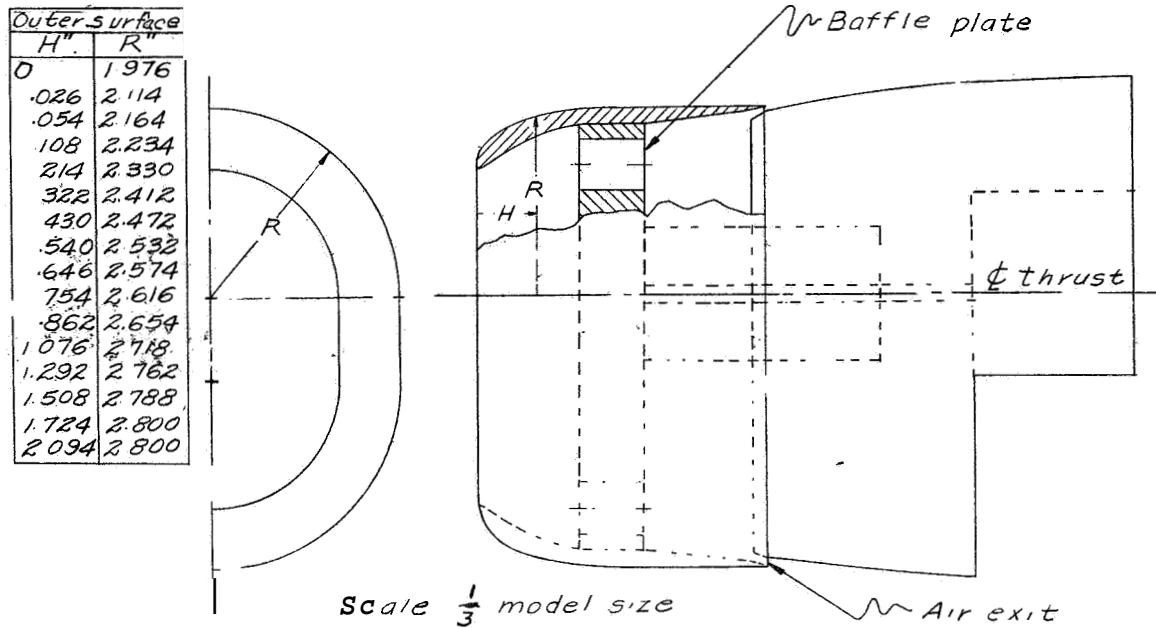


Figure 3 - Test arrangement for NACA open-nose cowl ng

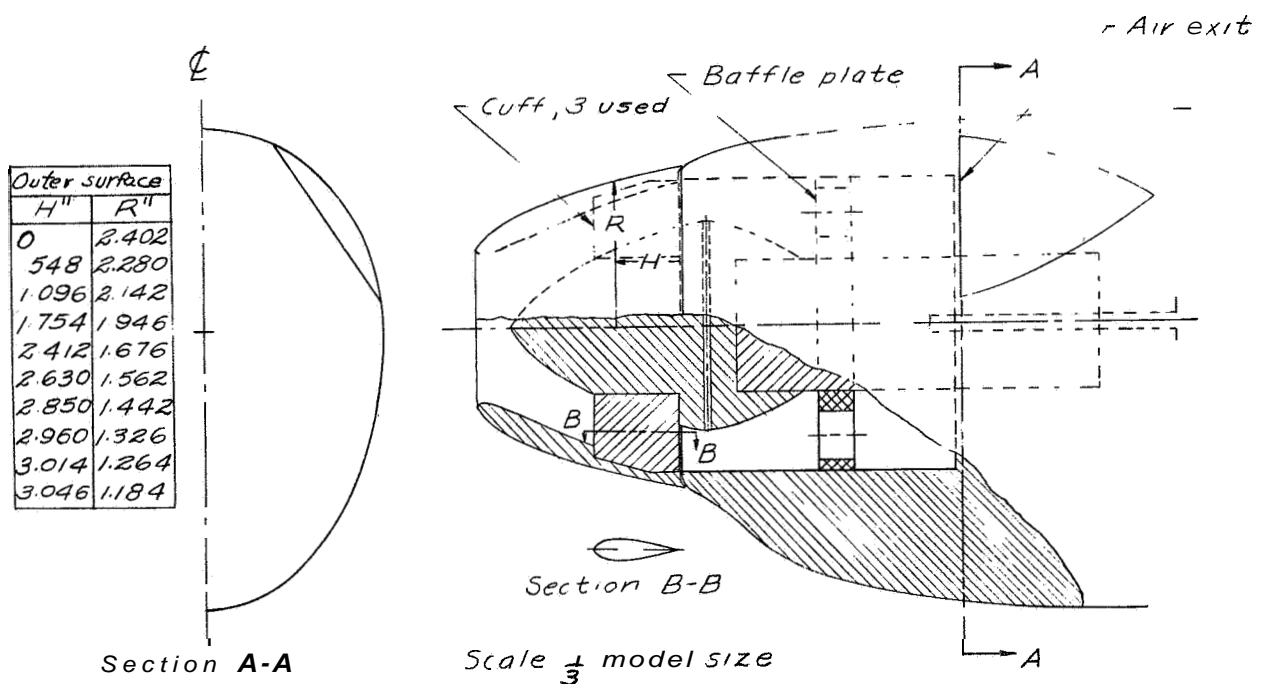
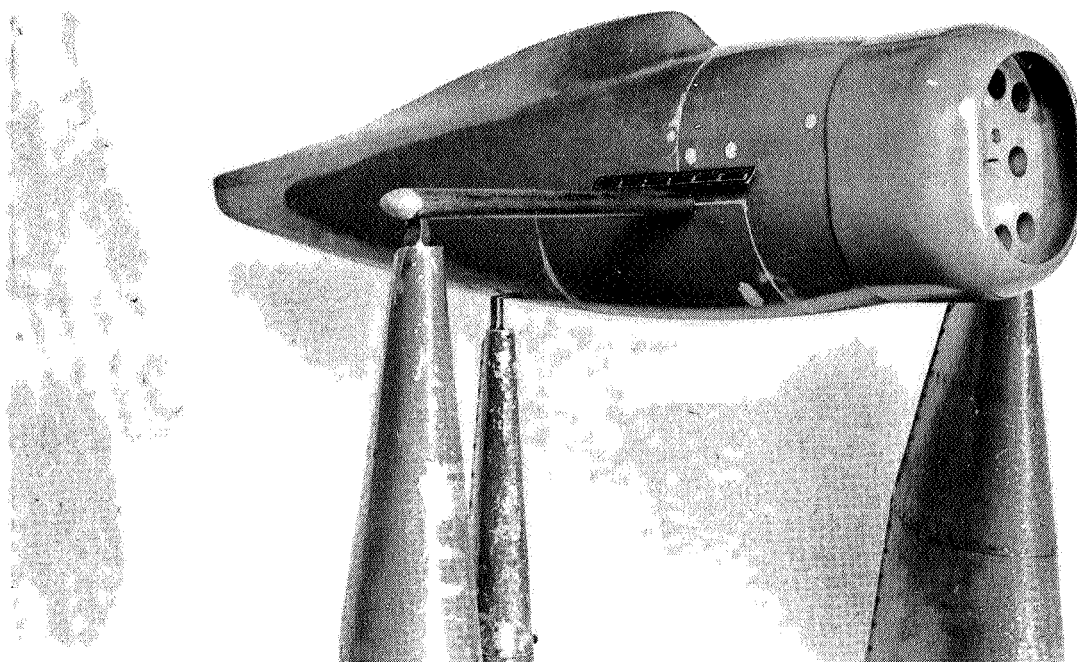
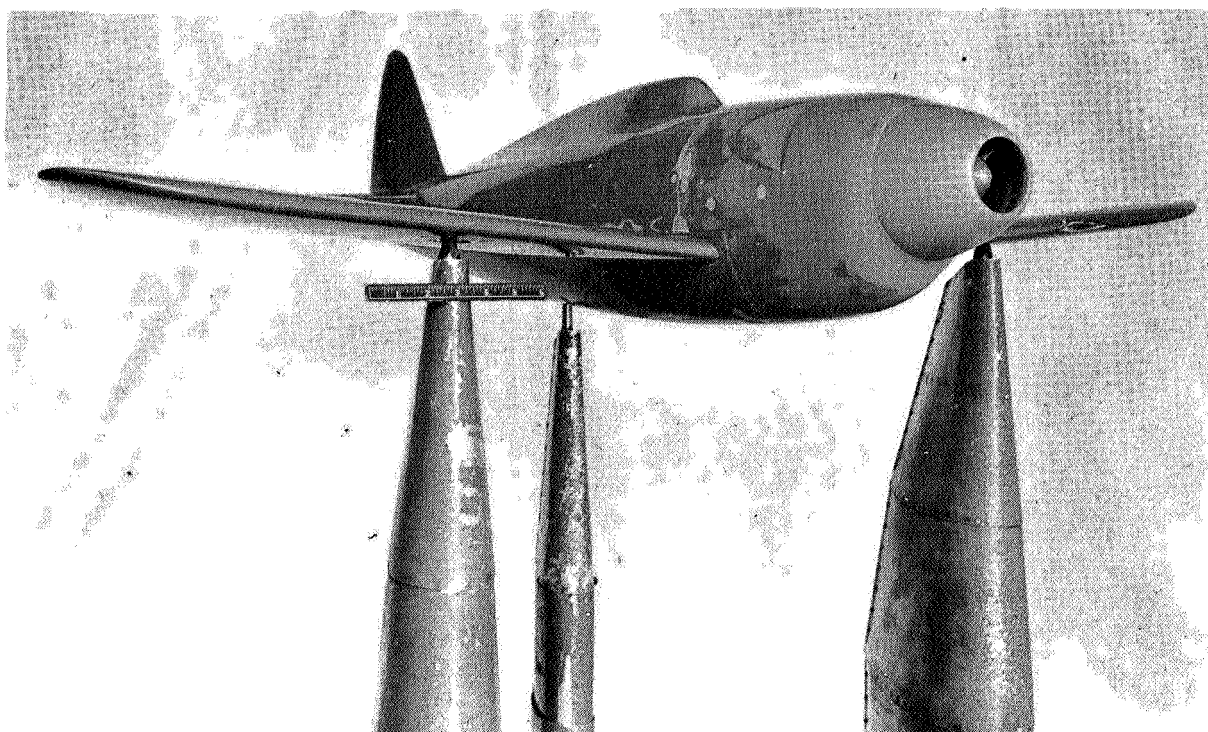


Figure 4 - Test arrangement of NACA high-speed cowl ng



(B) FUSELAGE WITH NACA OPEN-NOSE COWLING.



(A) COMPLETE MODEL WITH NACA HIGH-SPEED COWLING.

FIGURE 5. - MODELS WITH TWO TYPES OF NACA COWLING MOUNTED ON SUPPORTS.

NACA

○ — NACA open-nose cowling
+ — NACA high-speed cowling

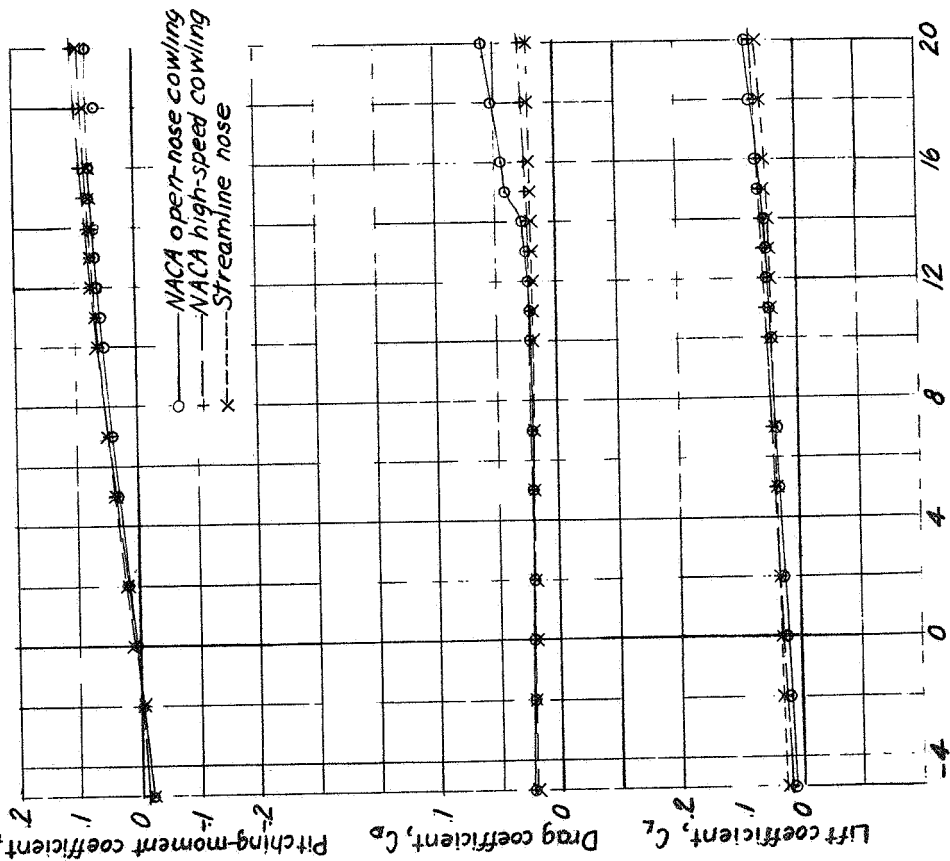
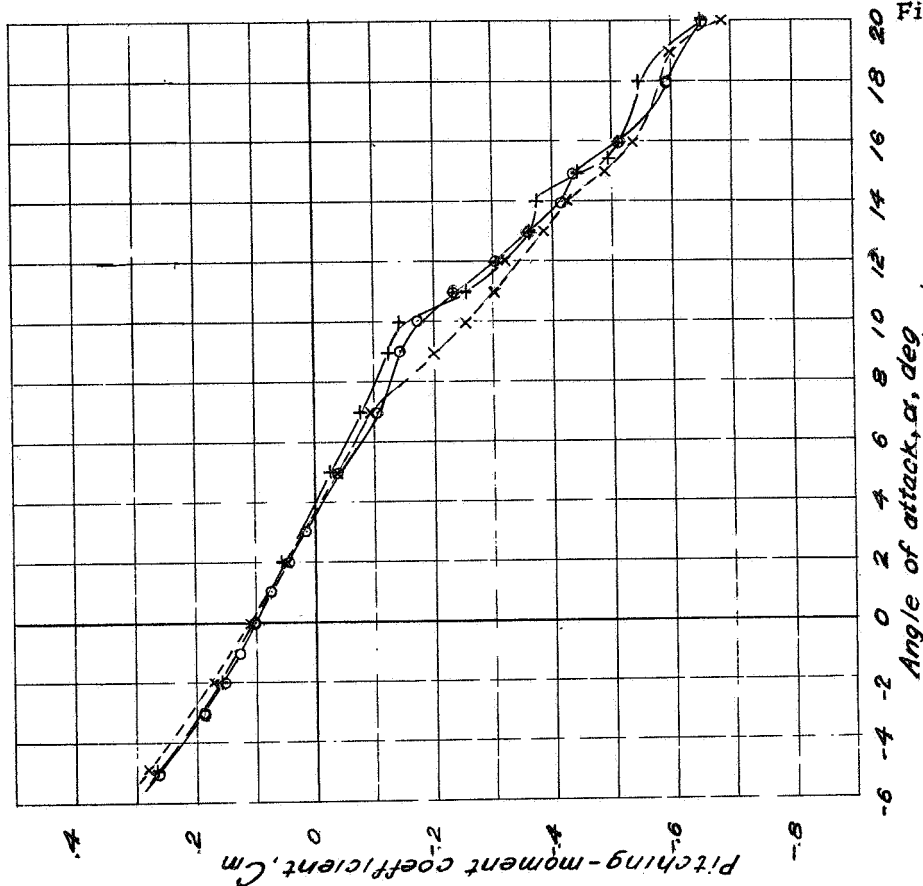


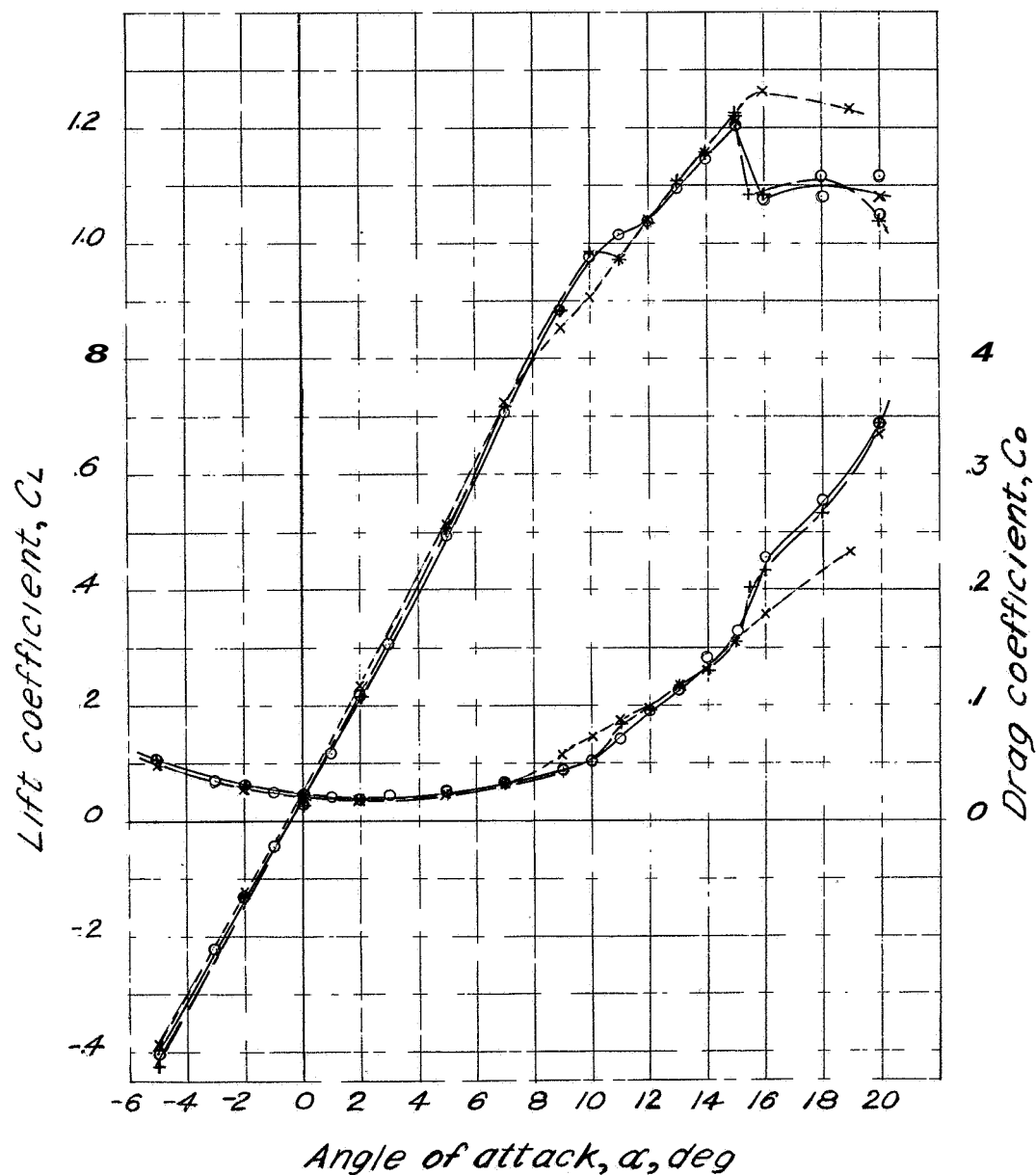
Figure 6.- Variation of lift, drag, and pitching-moment coefficients with angle of attack. Fuselage alone; α , maximum, ψ , 0.



(b) Pitching-moment coefficient
Figure 7.- Concluded.

Figs. 6, 7b

- — NACA open-nose cowl
 + — NACA high-speed cowl
 x — Streamline nose



(a) Lift and drag coefficients.
 Figure 7.—Aerodynamic characteristics of complete model, K ,
 maximum; η , 0.

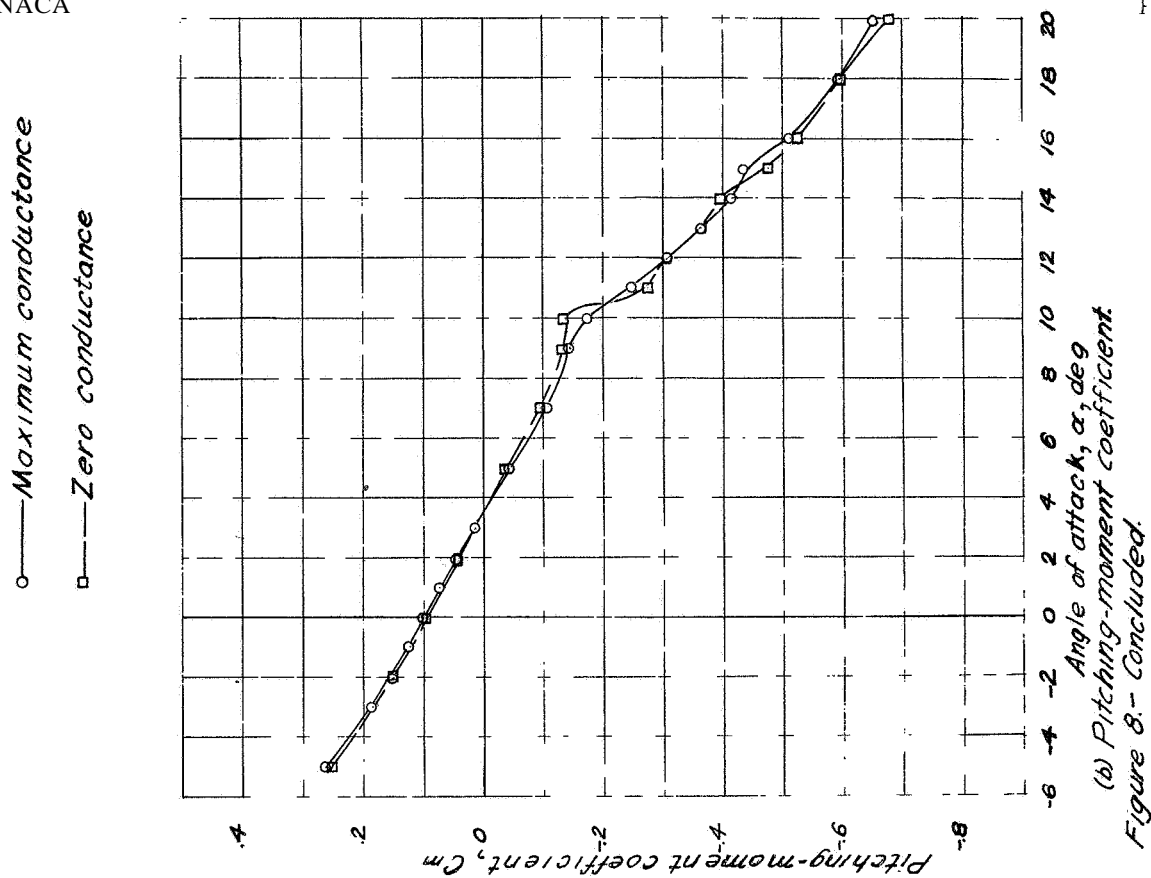
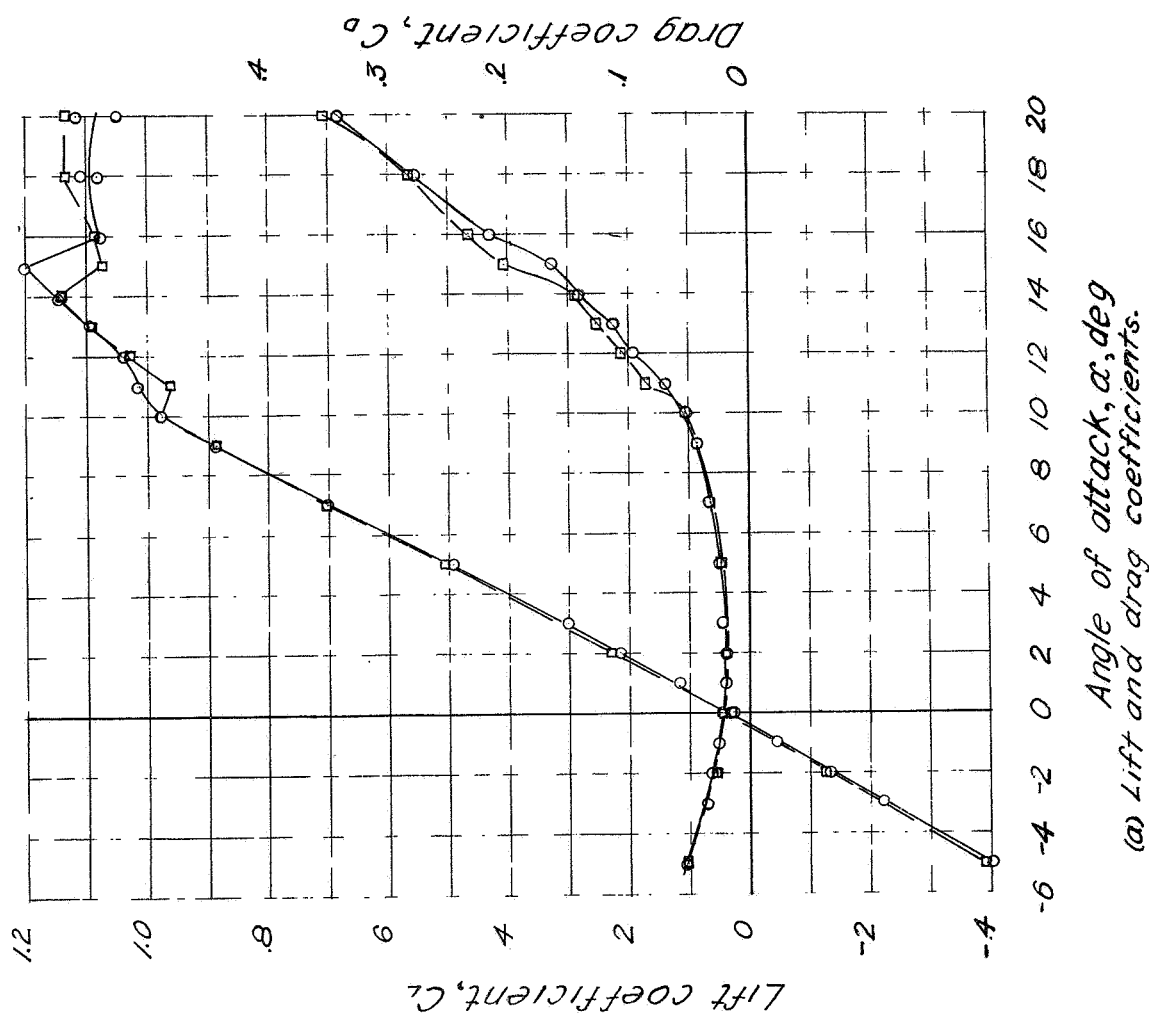


Figure 8.- Effect of conductance on aerodynamic characteristics of complete model NACA open-nose cowling; ψ , 0.

NACA

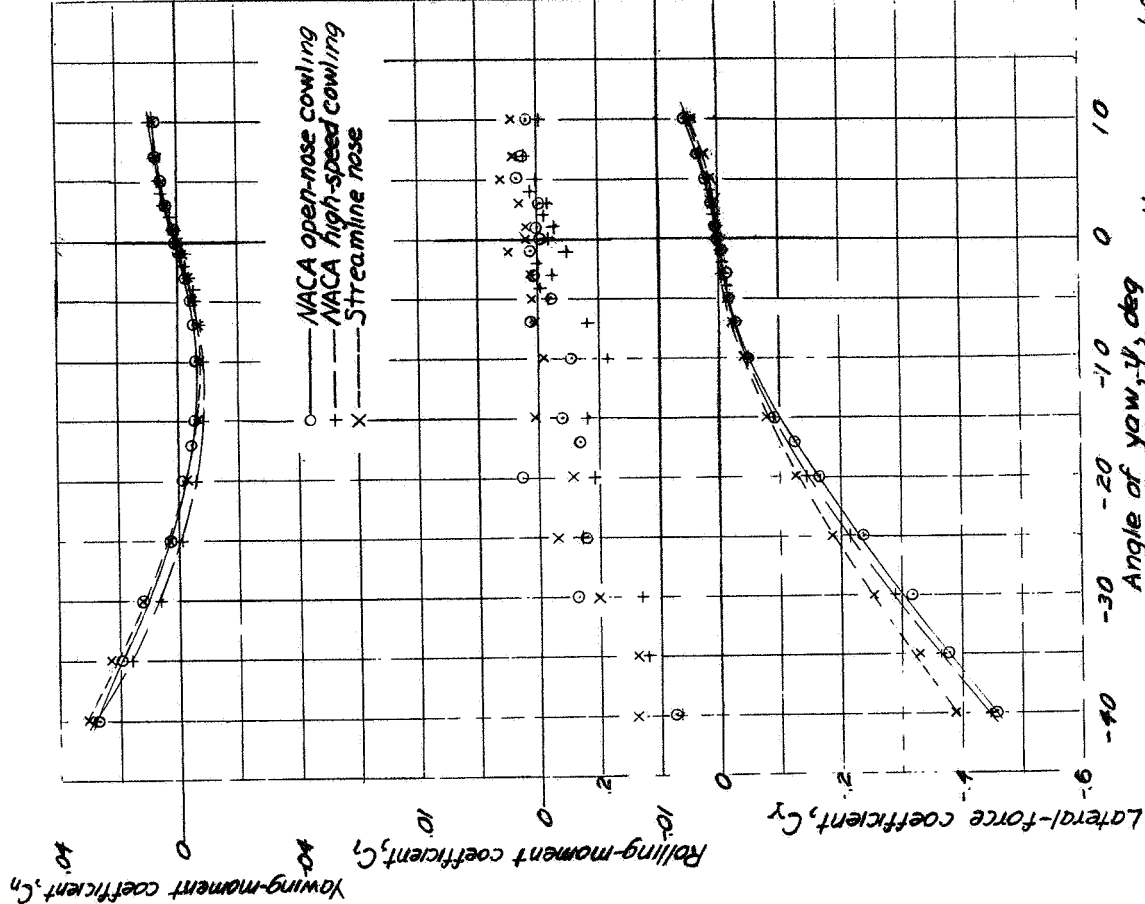


Figure 10.- Variation of lateral-force, rolling-moment, and yawing-moment coefficients with angle of yaw. Fuselage alone; K , maximum; α , $^\circ$.

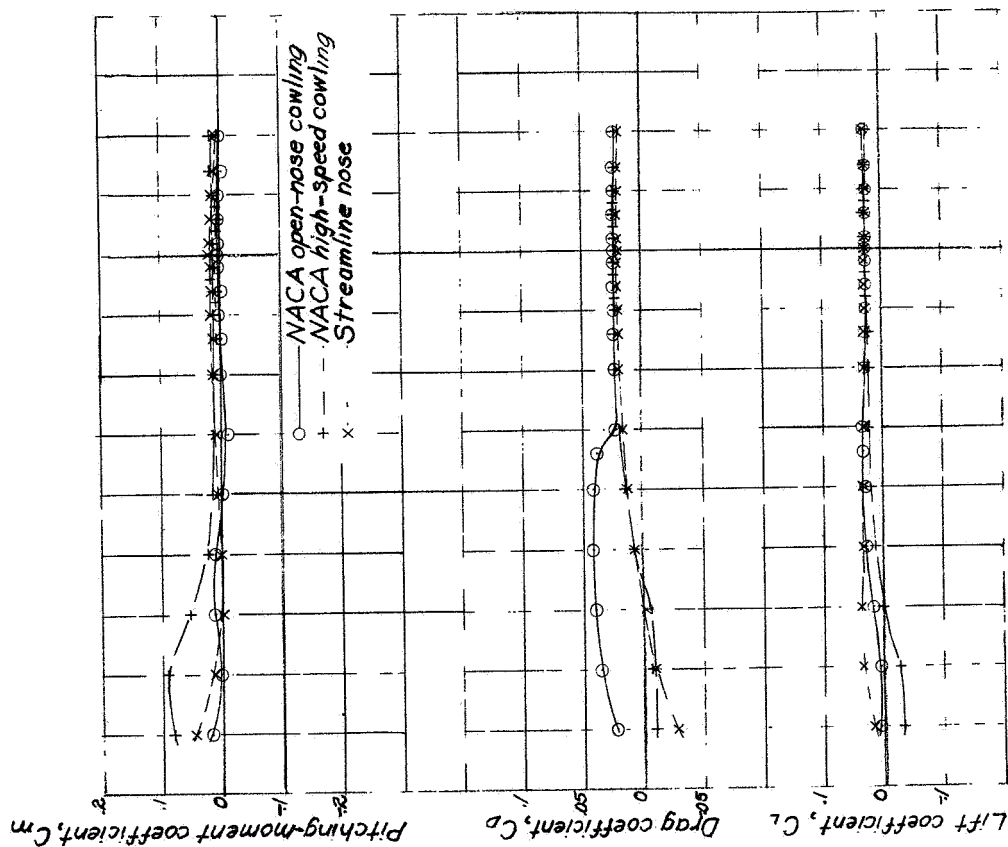


Figure 9.- Variation of lift, drag, and pitching-moment coefficients with angle of yaw. Fuselage alone; K , maximum; α , $^\circ$.

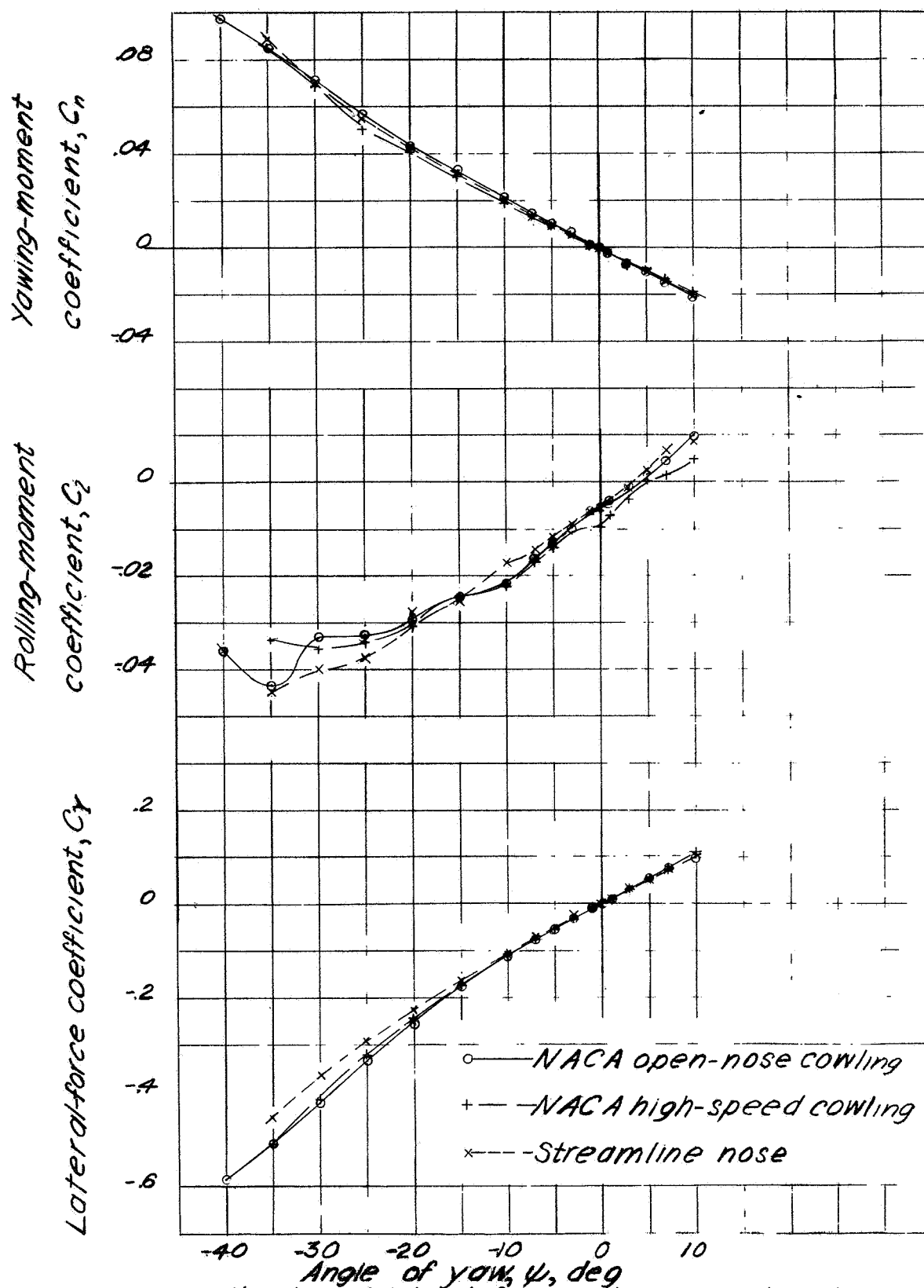


Figure 11.- Variation of lateral-force, rolling-moment, and yawing-moment coefficients with angle of yaw. Complete model, K , maximum; α , 0.

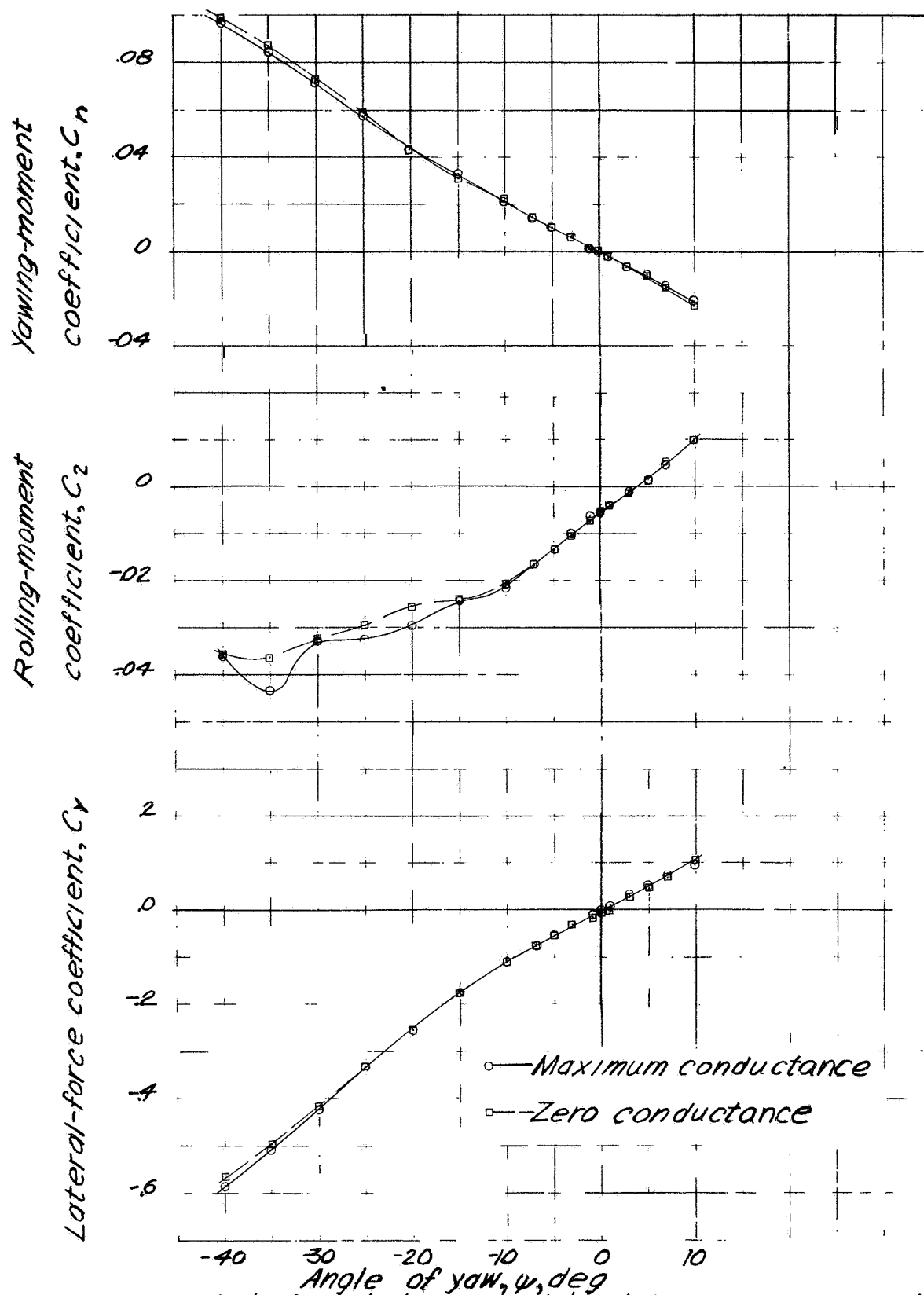


Figure 12.—Effect of conductance on lateral-force, rolling-moment, and yawing-moment coefficients. Complete model, NACA open-nose cowling; α , 0.

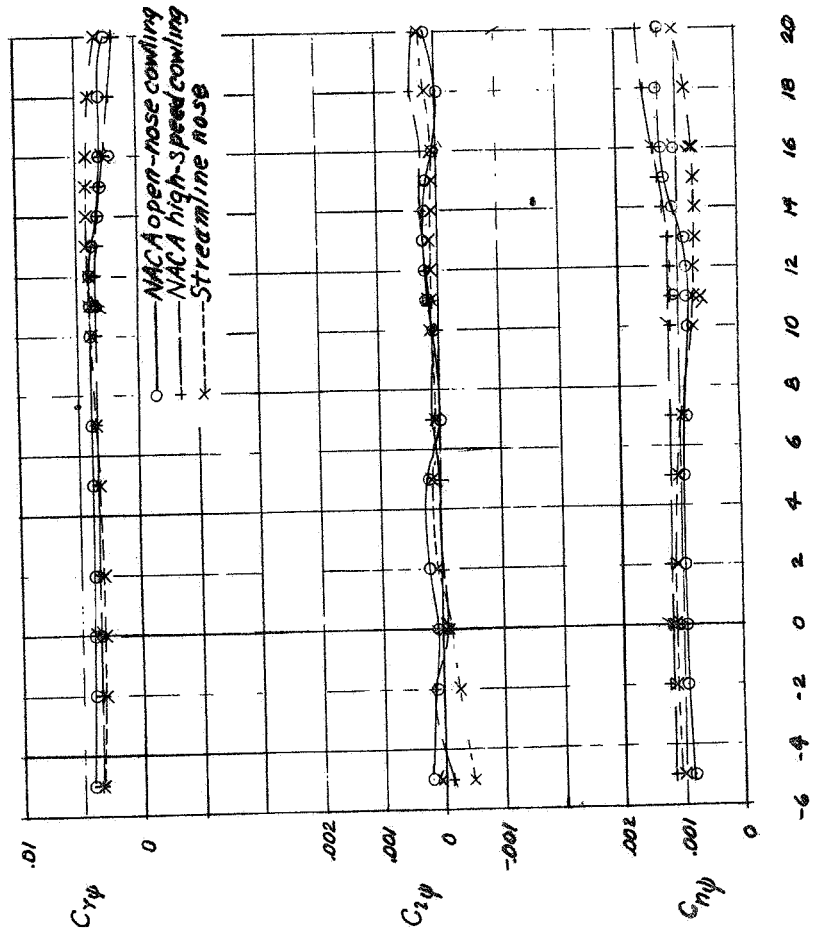


Figure 13.- Variation of C_L , C_D , and C_M with angle of attack. Fuselage alone, K , maximum.

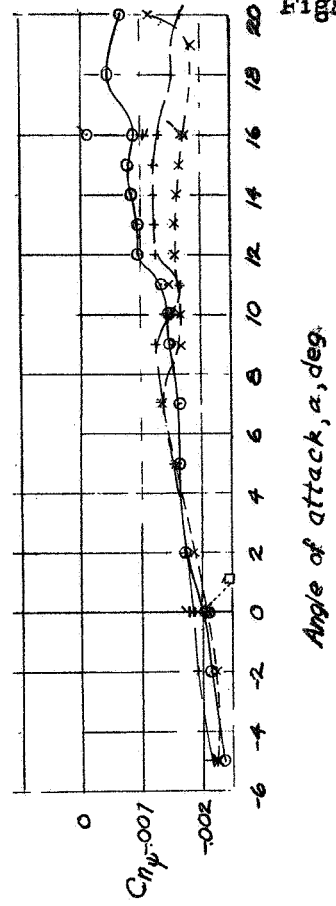


Figure 14.- Variation of C_L , C_D , and C_M with angle of attack. Complete model.